Direct injection supersonic cluster beam source for FT-ICR studies of clusters

Shigeo Maruyama,[a] Lila R. Anderson, and Richard E. Smalley
Rice Quantum Institute and Departments of Chemistry and Physics, Rice University, Houston, Texas 77251

(Received 26 July 1990; accepted for publication 20 August 1990)

A miniaturized pulsed supersonic beam source has been developed using laser vaporization of a computer-controlled target disk, producing intense beams of cluster ions with excellent repeatability and control. Due to its small size and narrow pulse width, the entire source is adequately pumped by a single 170 ℓ/s turbopump. The resultant vacuum quality permits this source to be attached to a Fourier transform ion cyclotron resonance apparatus (FT-ICR) such that the supersonic cluster ion beam is directly injected. The result is a powerful but simple FT-ICR instrument of wide applicability. The new source is suited as well for a variety of other uses such as molecular beam epitaxy.

I. INTRODUCTION

Fourier transform ion cyclotron resonance (FT-ICR) is one of the most powerful techniques of modern mass spectrometry. Over the past decade a number of methods were pioneered for the extension of this technique to the use of external sources. McIver *et al.* were the first to succeed in connecting a standard electron bombardment ionization source to a FT-ICR through the use of long quadrupole ion guide (rf only).[1,2] Shortly thereafter Alford *et al.*[3,4] and Kofel *et al.*[5,6] independently demonstrated that a simple einzel lens system would suffice as long as the ion beam was restricted to a narrow conical region centered around the central axis of the magnetic field of the ICR trap. For metal and semiconductor clusters this technique has opened up a vast array of new experiments.[7–11] Irion, Selinger, and Wendel have recently succeeded in coupling a Xe^+ sputtering source to an FT-ICR via an einzel lens system[12] and have published results of initial studies on a variety of metal clusters. Applications of these external ion source techniques have been increasing for the study of other species as well; one fine example being the recent adapting of an external Cs^+ secondary ion source to FT-ICR by Ijames and Wilkens;[13] another being the successful trapping, thermalization, and accurate (4 parts in 10^8) mass measurement of antiprotons generated by the 3.8-GeV proton synchrotron at CERN and temporarily held at 175 MeV in the LEAR storage ring[14]—certainly the largest external ion source ever used for an ICR apparatus.

This article describes what may be the smallest external ion source yet used with an FT-ICR apparatus. Because of its small size, it is readily pumped with a single small turbopump. The resultant high-quality vacuum properties of the source then allow it to be mounted directly on the magnetic axis of the superconducting magnet of the FT-ICR. Although primarily designed for the production of metal and semiconductor clusters, we believe it may prove to be highly valued for the production and FT-ICR study of a wide variety of molecular ions and complexes, including peptides, nucleic acids, and other large biopolymers. With small modifications this compact laser vaporization supersonic beam source may have many other uses beyond FT-ICR experiments. In particular it offers an intriguing alternative to the current hot-oven metal and semiconductor atom beam sources used in molecular beam epitaxy (MBE).

II. EXPERIMENT

Figure 1 displays a schematic cross section of the new compact cluster beam source. It has evolved from the earlier work in this laboratory on supersonic beam sources based on laser vaporization of a rotating, translating target surface mounted on the front of a pulsed supersonic valve.[15] In particular, it is a direct outgrowth of a new design philosophy for laser vaporization cluster beam sources developed for the study of argon complexes of carbon clusters such as C_{60} (buckminsterfullerene).[16] The key feature of this new philosophy is that it is best to fire the vaporization laser on the leading edge of the rising carrier gas pulse. Otherwise a well-defined shock wave forms in the high-density carrier gas above the target as the laser-vaporized plume begins to expand. Since this shock wave cannot travel much faster than the speed of sound in the carrier gas at the initial temperature of the nozzle, the vapor plume is effectively confined for several microseconds. For materials such as carbon which condense easily at high temperatures, this confinement results in most of the material emerging in the form of macroscopic aerosol particles, with little if any net yield of clusters in the 1–1000 atom size range. With the straightthrough flow design of the standard laser-vaporization nozzle source,[15] the only solutions available to this problem were either to make use of turbulence to sweep off the top corona portion of the laser-induced plasma plume where some free atoms and small clusters were still present, or simply to use less carrier gas.

[a]RQI Visiting Fellow. Permanent address: Department of Mechanical Engineering, University of Tokyo, Bunkyo-ku, Tokyo 113, Japan.

 0034-6748/90/123686-08$02.00

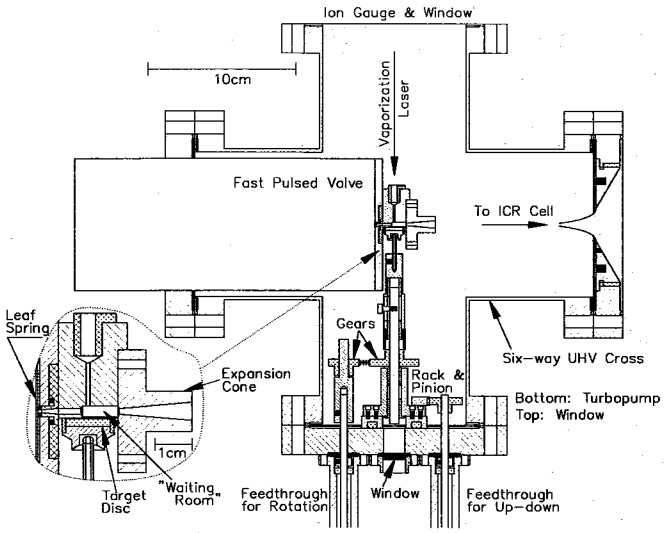

FIG. 1. Horizontal cross-sectional schematic of the compact pulsed supersonic cluster beam source using laser vaporization of a target disk that is rotated and translated under computer control.

Neither of these options is entirely satisfactory for a general purpose supersonic cluster source. Nozzle operations based on turbulence are intrinsically unstable since the exact geometrical details of the nozzle region around the point of vaporization change as the target surface becomes eroded. On the other hand, using less carrier gas usually results in the clusters being inadequately cooled and not receiving sufficient collisions during the supersonic expansion to attain the full terminal velocity.

Instead, we have pursued the alternative of using an extremely fast-rising carrier gas pulse, and postponing this gas pulse as late as possible after the vaporization laser has fired. This allows the vapor plume to expand unimpeded for a while before it is entrained in the rising density of the carrier gas pulse. Such operation on the leading edge of a fast-pulsed carrier gas flow is the basis of the new design philosophy now in use throughout our laboratory in all our suprsonic cluster beam machines.[16-18]

The pulsed nozzle used is of the magnetic "current loop" variety first proposed by Dimov,[19] and applied to supersonic molecular beam experiments by Gentry and Giese.[20] Ironically, a crude version of this current loop technology first implemented in our laboratory for laser spectroscopy of cold molecules and radicals[21] was actually used in the very first experiments in laser-vaporization production of cluster beams.[15a] Although we soon abandoned these fast pulsed nozzles in favor of double solenoid designs capable of much higher gas flows,[22] we have now become convinced that this was a mistake. Although the current loop design delivers less total gas flow per pulse, with a suitably miniaturized nozzle design the same high peak pressures may be obtained in the nozzle in a much more useful time regime.

With the designs currently in operation on our cluster tandem time-of-flight,[16] and ultraviolet photoelectron spectroscopy[17,18] apparatuses where a double version of these current loop pulsed nozzles have been in operation over the past year, we have routinely generated more intense, well-cooled supersonic metal and semiconductor cluster beams than was ever reliably available from the older nozzle technology.

In the cluster source shown in Fig. 1 the prime objective was to keep the source compact and highly reliable. Since the clusters would have to be cooled in any event after they entered the FT-ICR trap, it was not necessary to use more than one pulsed valve to achieve the necessary carrier gas density. Although it descended directly from our original current loop design,[21] the pulsed valve used in this new cluster nozzle is adapted from a much improved version now available commercially.[23] It is the "fast pulsed valve" shown in brief outline in Fig. 1. This valve uses a gold-plated beryllium-copper leaf spring clamped to seal over the top of a 0.07-cm-i.d. viton O-ring. As installed, the fundamental up-down flexing vibrational mode of this spring has a frequency of roughly 4 kHz. When a 20-μs current pulse is applied along the length of the spring the associated magnetic field repels a corresponding field generated from a return conductor mounted underneath, generating an effective impulse to excite the spring vibration. At some point in the upward travel of the center of the spring, the seal with the O-ring is broken and gas begins to flow through the valve, the flow continuing until near the end of the first half-cycle of the harmonic spring vibration when the seal with O-ring is re-established. The exact opening and closing time of the valve is a function of magnitude of the current pulse that drives the valve, the gas pressure in the valve, the valve temperature, and the mechanical adjustment of the O-ring compression. Once these parameters are set, however, the timing of the valve is quite reproducible since it relies on what is effectively an impulse excitation of a simple mechanical resonance. The driving circuitry is controlled so that the spring is never driven past its elastic limit.

This mechanical resonance aspect of the magnetic current loop pulsed valve design is vital to the successful operation of the entire cluster beam apparatus. As long as the spring is neither overheated nor overdriven, its fundamental flexing frequency is constant. This provides the timing reproducibility that is so critical in reliably synchronizing the laser vaporization event with the rising edge of the gas pulse within an error of a few microseconds.

A. The supersonic nozzle and its "waiting room"

Once the fast pulsed valve is open, the carrier gas passes through the 0.07-cm-i.d. main sealing O-ring and flows down a 0.5-cm-long conical tube machined in the O-ring mount, increasing from 0.07-cm-i.d. at the base of the O-ring to 0.15-cm diameter at the exit. This gas pulse then passes into the 0.15-cm-diam entrance tube of the nozzle block shown bolted to the front of the fast pulsed valve in Fig. 1, and seen in more detail in the expanded view of this figure. After a 0.6-cm straight length of this entrance tube, the gas expands into a 0.3-cm-i.d., 1.0-cm-long cylindrical "waiting room" which is the zone in the nozzle where the clusters are formed and thermalized. The

main flow of the carrier gas then passes through the 0.15-cm-i.d. entrance of a 2.0-cm-long conical expansion cone, 10° total internal angle. As seen in Fig. 1, the gas can then undergo a free supersonic expansion, the central 0.2-cm-diam section of the jet being skimmed at a distance of 8.4 cm downstream by a 2.1-cm-long electroformed nickel skimmer[24] with 25° total internal angle at the orifice.

As shown in Fig. 1, the vaporization laser beam (second harmonic of a Nd:YAG, 10–30 mJ pulse^{-1}, 5-ns pulse length, focused to a 0.07-cm-diam spot) is directed through a 0.1-cm-diam entrance hole drilled in the 304 stainless-steel nozzle block. The vaporization laser beam passes through the "waiting room," through a 0.1-cm-diam hole on the opposite side, and hits the target disk. The cross-hatched insert piece on the entrance to the vaporization laser access hole is machined of Teflon. Its outer surface is canted so that coarse misalignment of the laser beam is easily visible on the white Teflon surface.

Milani and deHeer[25] recently described a new laser vaporization cluster source that has some aspects in common with the one described here. They too discovered the importance of what we have called the waiting room. However, with the more complicated flow path and slower pulsed nozzle used in their valve, they were unable to attain sufficiently high carrier gas pressure at the moment of laser vaporization to accelerate the clusters to the full terminal velocity of the supersonic beam.

B. Target disk mounting and motion control

Also evident in Fig. 1 is the disk rotation and translation mechanism, which has received a great deal of detailed attention in this design. After many years of experiments with various laser vaporization cluster beam devices, the experience of this laboratory has been that the vaporization target quality and positioning is the single most troublesome aspect. With this compact source with its small target disk nozzle flow regions, this target problem is expected to be even more extreme. In order to obtain the necessary control the new source has relegated this responsibility entirely to computer control via stepping motors. The mechanical assembly shown in Fig. 1 and described briefly below achieves these requirements nicely, with an overall repositioning accuracy under computer control of better than 0.01 cm.

The disks used with this source are 1.2 cm o.d. Depending on the material, they are either precut on a lathe or sanded to the appropriate o.d. after being epoxied to the small aluminum mount shown in the Fig. 1. The seal to the nozzle block is made by a Teflon ring 0.1 cm thick that slides over the outside of the target disk and seats further back on the aluminum mount. After assembly this Teflon ring is carefully sanded down so that the clearance between the surface of the target disk and the nozzle block is on the order of 0.003 to 0.010 cm. The Teflon ring can easily be removed later, after the disk has been worn down by extensive laser vaporization, permitting the disk surface to be ground smooth for reuse. The same Teflon ring then may be reused as well, with only a slight sanding to readjust the gap.

The aluminum disk mount is manipulated by a "ball driver" which fits into the head of a socket head screw epoxied into the rear of the mount. As shown in Fig. 1, this ball driver shaft is held in a mount that slides over an angular locating pin on a central axle that can be rotated by an external rotary motion feedthrough, connected to this feedthrough by a nonslip polyurethane drive belt running between two sprocket gears. The ball driver mount is forced forward by a spring mounted on the rotation shaft, thereby pressing the disk mount against the nozzle block.

Some study of Fig. 1 will show that this central rotation axle itself is held in a block that is bolted on either side to two linear ball-bearing slides that permit the axle block to travel up or down (note: the view of this figure is from the top looking down; up/down motion is therefore perpendicular to the page). The position of the rotation axle block on this linear slide is determined by a second rotatory vacuum feedthrough operating via a rack-and-pinion linkage.

One of the most critical parameters to monitor in these laser vaporization devices is the precise alignment of the laser through the nozzle block. Figure 1 shows that there is an alignment window mounted on the vacuum wall immediately behind the central rotation axis. When desired, the computer may be directed to move the disk out of the way, clearing the central laser axis so that the vaporization laser beam passes through the entrance and exit windows of the entire cluster source. Precise alignment is then easily achieved by monitoring the shape of the transmitted laser beam.

While operating the cluster source the target disk is moved to a fresh spot prior to each vaporization laser pulse. Generally the distance moved is calculated so that the laser ablation of the disk is uniform, regardless of the radius. The ability to do this so precisely under computer control is a primary reason why this cluster source produces such reproducible beam pulses with little shot-to-shot variation over many days operation on a single target disk.

C. Turbopumps and direct connection to the FT-ICR apparatus

As is evident in Fig. 1, one of the principle advantages of this new source is that it is small enough to fit entirely within a standard 15-cm-o.d. conflat flange six-way UHV cross. Since the volume of this UHV cross is small (3 ℓ), a 170-ℓ s^{-1} turbopump is adequate to pump it out in between beam pulses at 10 Hz. Operating with helium at a backing pressure of 10 atm, the pulsed valve used in this source is capable of putting out 0.05 Torr ℓ in a 125-μs pulse. In this 3-ℓ chamber such a fast pulse will temporarily raise the pressure to 2×10^{-2} Torr, which would ordinarily be completely unacceptable in a cluster beam machine operating with diffusion pumps. However, for short periods of time this is not a problem for the small turbopump.

The fast rise time of the pulsed valve and precise synchrony with the vaporization laser allow the entire process of generating a cluster beam pulse to occur in less than 100

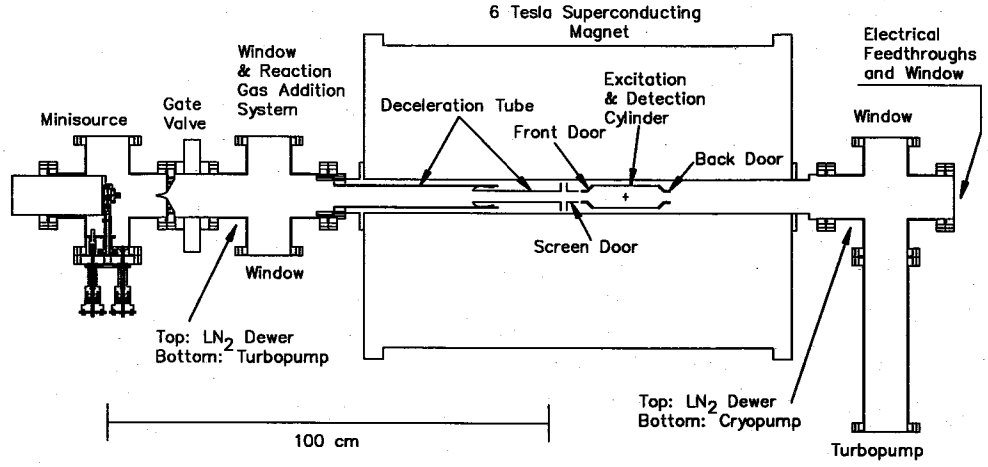

FIG. 2. Schematic view of FT-ICR apparatus with direct injection of clusters from the compact supersonic cluster beam source.

μs. Even with helium as a carrier gas this is such a short time that the shock waves coming back off the interior walls of this small vacuum chamber cannot interfere with the beam pulse. The result is that the cluster source is well balanced: it has about the right size for the pulse duration of the beams that will be produced. The longer pulses of previous solenoid nozzle designs would have required a considerably larger chamber, which in turn would not easily be handled by turbopumps.

In operation with a helium carrier at 10 Hz with a 0.05 Torr ℓ per pulse gas output, the average pressure in this source is roughly 4×10^{-3} Torr; but with the pulsed valve turned off the background pressure drops into the low 10^{-7}-Torr range within a few seconds, and below 5×10^{-8} Torr after 15 s. Given the high reliability of the pulsed valve and the nozzle translation/rotation vacuum feedthroughs, the vacuum aspects of this cluster source are sufficiently safe that it may be attached directly to a wide variety of UHV-sensitive machines. Figure 2 shows it attached directly to the bore tube of an FT-ICR apparatus featuring a 6.0-Tesla superconducting magnet with a 7.5-cm-i.d. room-temperature bore.

D. FT-ICR details

The fine points of this FT-ICR apparatus were much the same as described in earlier publications from this group.[8,10] The ICR trap was centered in the homogeneous region of the magnetic field where the radial ion motion was confined by the magnetic Lorentz force which determines the cyclotron motion. Along the magnetic central axis the confinement of the cluster ions in the trap was accomplished by two conical-shaped electrodes—the "front" and "back" doors labeled in Fig. 2. Note that the doors had large (2.5 cm i.d.) holes in the center to permit the clusters to pass through whenever permitted by their axial energy. These holes also allowed free passage of laser radiation without scattering. The side plates of the ICR trap were composed of four sectors of a 4.8-cm-i.d. cylinder, 15.0 cm in length. Two opposing 120° sectors were used for rf excitation of the trapped cluster ions, while the other two 60° sectors were used for detection of the image current induced by the cyclotron motion.

In front of the front door was a "screen" door that was mounted close to a two-part tubular structure labeled the "deceleration tube." These two parts of the deceleration tube were connected together by a flexible wire in the center, and to an external voltage pulser through a connection at the front (source) side. Positively charged clusters traveling through the middle of this tube were effectively decelerated as they passed to the "screen" door because the decelerator tube was pulsed to a negative potential while they were still inside and experienced (due to Gauss's law) no field in this nearly closed conductor before they attempted to "climb out" of the decelerator tube to get back to ground potential at the screen door.

Unlike previous versions of this cluster FT-ICR apparatus, this "screen" door actually has no screen. Instead, it simply has a 2.5-cm-i.d. clear internal aperture in order to eliminate any problem with scattered laser light in experiments requiring intense excitation of the trapped clusters. This absence of real screens does have the effect that the deceleration field formed between this door and the end of the deceleration tube has a slight curvature. But at the moderate fields used with this direct injection cluster beam source, SIMION[26] calculations show that this field curvature produces only a slight amount of cyclotron excitation as the cluster ions pass through to the trap.

As shown in Fig. 2, entrance and exit to the bore tube of the FT-ICR magnet was connected to two 15.0-cm-flange-diam six-way crosses, each of which was pumped by a separate 170-ℓ s^{-1} turbopump. In addition, the last cross was pumped by a 20.0-cm-i.d. CTI cryopump that was valved off under computer control by a single-vane butterfly valve during the injection cycle. Ordinarily, for the experiments reported here the pressures recorded near these six-way crosses on either side of the FT-ICR bore tube when the cluster beam source was off were in the low 10^{-9} Torr range.

As described in other recent publications from this group, excitation and manipulation of the cluster ions in the ICR trap involved extensive use of computer-generated rf waveforms to insure the desired rf power spectrum was being applied. The ICR transients were detected by a Stanford Research Systems model SR560 preamplifier, fol-

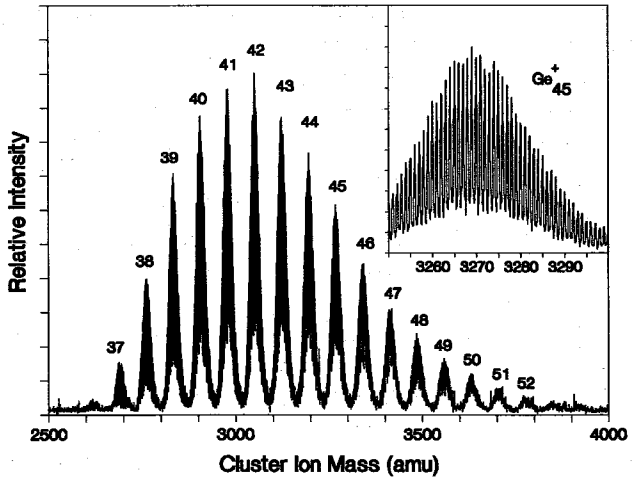

FIG. 3. FT-ICR mass spectrum of germanium clusters as injected by the pulsed supersonic cluster source. The insert panel is an expanded view showing the isotopic composition of the Ge_{45}^{+} clusters in the ICR cell.

lowed by 12-bit digitization and relatively straightforward FFT data processing[27] to produce the mass spectra shown below.

Although the experiments discussed here may appear complex, we emphasize that most of what is being used is actually just commercial hardware strung together with a few simple extra parts.

III. RESULTS

Figure 3 displays a typical FT-ICR mass spectrum of positive cluster ions directly injected using the new source with a germanium target disk. For this experiment the vaporization laser was fired 110 μs after the peak of the current pulse driving the spring of the pulsed valve. Previous experiments with this nozzle attached to a time-of-flight (TOF) mass spectrometer that could sensitively monitor the time evolution of the cluster beam pulse, had shown this timing to correspond to roughly halfway up the rising edge of the gas pulse into the "waiting room" (WR) of the nozzle as shown in Fig. 1. With the nozzle dimensions used in this experiment, we estimate that the helium gas pressure in the nozzle at the moment of laser vaporization was roughly 200 Torr, and that the average residence time of the clusters in the WR was 40 μs, during which time the pressure should have increased to 400 Torr. Measurements of the cluster ion arrival time distribution with the TOF mass spectrometer verified the expected 40 μs width of the ion packet, and showed that there was a slight (roughly 10%) slippage of the arrival time of the heaviest clusters to later arrival times.

These conditions were chosen to optimize the yield of germanium cluster positive ions produced by the source. Since ionization here is only the residual amount left after recombination of the original laser-induced plasma, these are not the optimum nozzle conditions for production of the most intense neutral cluster beam. The various modes of operation of these fast-pulse laser vaporization sources has been discussed in detail elsewhere.[16] For the bulk of the ICR experiments of interest with positive and negative clusters, this mode of using the residual ionization from the laser vaporization event is quite adequate.

Since the germanium cluster ions are all accelerated to nearly the same 1.9×10^{5} cm s^{-1} velocity by the supersonic expansion, each cluster has a translational energy that is linearly dependent on its mass. This fact permits a coarse selection of the range of clusters to be trapped in the ICR cell simply by controlling the deceleration voltage. In the example shown in Fig. 3 the deceleration tube was pulsed to -45 V after a 450-μs delay from the vaporization laser pulse to allow the clusters sufficient time to pass deep into the tube while it was still as ground potential. As the cluster ion packet neared the end of the deceleration tube 110 μs later, the screen door was pulsed from 10 V down to 0 V and held there for 80 μs, allowing the cluster ion packet to pass through as it decelerated. During the injection cycle the front door of the ICR cell was held at 4 V and the rear door at 10 V.

If the ion velocity had been exactly 1.9×10^{5} cm s^{-1} for all clusters in the beam, these injection conditions should have trapped only those clusters in the size range from Ge_{36}^{+} to Ge_{41}^{+}. As seen in the figure, the actual trapped cluster distribution is a bit wider, and shifted to heavier clusters than predicted by roughly 10%. Much of this is a consequence of the small velocity slippage of these large clusters from the full terminal velocity of the supersonic beam.

Another major factor contributing to this broader than expected trapped cluster ion distribution is the axial component of the Lorentz force the cluster ions experience as they enter through the divergent fringing field of the magnet. With the 0.2-cm-i.d. skimmer used in this source the bulk of the supersonic beam lies within a divergence of 10 mrad. By careful mechanical alignment of the cluster source with the magnet we have insured that this small diameter, well-collimated supersonic beam is very close to the central axis of the magnetic field where the magnetic mirror effect is minimal. Even so there is still some interaction. Full numerical simulations of the injection of these ions through our magnet show the maximum conversion of axial-directed translational energy into cyclotron motion upon injection to be roughly 10%. This contributes to the shift to higher-than-expected masses and does much to explain the observed asymmetry of the trapped ion distribution evident in Fig. 3.

In order to produce the mass spectrum of Fig. 3, the injection process was repeated 10 times over a period of 1 s. During this time the average helium pressure in the region of the ICR cell was estimated to be in the range of 10^{-4} to 10^{-3} Torr, with the peak pressure rising to 10^{-2} Torr immediately after each supersonic beam pulse. Since the cluster ion packet arrives at the ICR cell within the first 50–100 μs of the supersonic beam pulse when the pressure is still quite low, this large average and peak gas load on the ICR is acceptable. Slower pulsed supersonic sources would have been unacceptable in this respect, however.

In accord with our normal operating procedure with

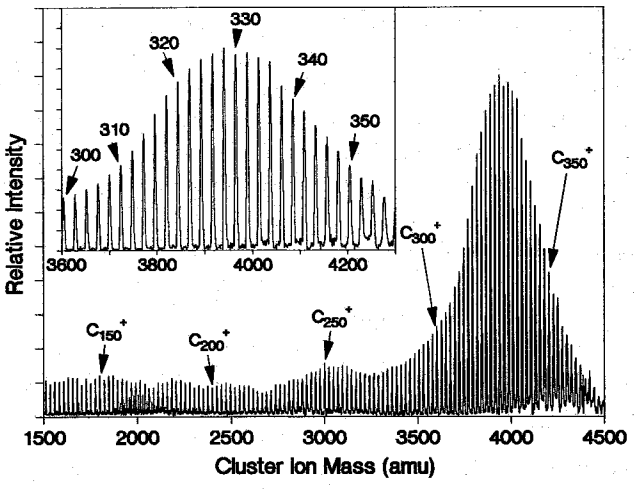

FIG. 4. FT-ICR mass spectrum of carbon clusters as injected from the pulsed supersonic cluster source. Note in the insert panel that only even numbered clusters are present. The small peaks near 2000 amu that appear to be due to the odd-numbered clusters actually result from the second harmonic of the ICR signal of the even-numbered clusters near 4000 amu.

supersonic cluster ICR,[7–11] after the injection process the front and rear door voltages were ramped to 10 V over a period of 1.0 s, and the clusters were then exposed to argon at a pressure of 2×10^{-5} Torr for 2–10 s in order to thermalize their motions in the ICR trap to near 300 K. The ICR transient was then excited with a computer-generated rf waveform having constant power over the frequency range of interest and resulting coherent ICR transient was detected and processed to produce the spectrum shown in Fig. 3.

FT-ICR mass spectra of metal and semiconductor cluster ions such as Fig. 3 have now been obtained for a wide variety of materials, including both pure elements such as the germanium used in Fig. 3, carbon,[28] silicon,[29,30] aluminum, and transition metals such as niobium and cobalt, as well as mixed systems such as gallium arsenide,[31] and carbon/potassium fullerenes.[28] In all cases the performance of the overall apparatus has been quite reproducible.

A. Carbon is an exception

The only exception encountered thus far to the general rule, that we trap clusters about 10% heavier than we would calculate, has been carbon. Operating the cluster ion source at the same time conditions used for the germanium cluster data of Fig. 3 gave only a slight signal for carbon clusters. Instead to achieve the optimum carbon cluster signal in the ICR as shown in Fig. 4, it was necessary to fire the vaporization laser 65 μs after the peak of the current pulse to the leaf spring of the pulsed valve —much earlier than normal. Due to delays in the movement of the spring to the point where the valve first starts to open, and the time it takes for significant gas flux to emerge into the WR, this laser vaporization time corresponds to a very early stage of the gas pulse above the target disk when the pressure in the WR is estimated to be roughly 50–100 Torr. This is a vivid demonstration of the virtues of operating on the rising edge of a fast-pulsed gas valve. Vaporization of carbon at higher pressures later in the gas pulse confines the laser-induced plasma to a smaller volume, and, in the case of carbon where condensation to clusters is extremely facile even at high temperatures, produces such a high cluster density that ion recombination and aggregation to form macroscopic aerosol particles is the dominant kinetic fate.

Note that only even-numbered carbon clusters are evident in the FT-ICR mass spectrum of Fig. 4. This is part of the mounting evidence that graphitic closed shells consisting of six-membered aromatic rings and 12 five-membered rings are formed with great facility whenever carbon condenses.[11,28]

As a consequence of operating at such an early stage in the gas pulse, even with the 40-μs mean residence time of the "waiting room," the carbon clusters still expand from the nozzle in a carrier gas that is hot (at low gas densities, the energy of the vaporization laser is dissipated over less gas particles, producing a higher temperature). Correspondingly, the optimum time for pulsing open the "screen door" to let the clusters into the FT-ICR cell for Fig. 4 was found to be reduced to 530 μs (compare to the 560-μs flight time used for the germanium clusters of Fig. 3). In this case of carbon clusters the decelerator and door voltages were set so that carbon clusters in the C_{330}^+ to C_{360}^+ mass range should have been trapped, assuming a beam velocity of 1.9×10^5 cm s^{-1}. Instead, as is evident in Fig. 4, the dominant distribution trapped under these conditions is roughly 10% smaller in mass. This is readily explained by the fact that the cluster beam is a bit faster than normal due to the fact that the effective source temperature was higher than room temperature.

However, the most significant exception to the expected narrow trapped mass range seen in the carbon clusters of Fig. 4 is the broad distribution of clusters evident with sizes smaller than 300 atoms. We have found this broad lower-mass distribution is basically independent of deceleration voltage in the new ICR apparatus. These relatively small carbon clusters in the size range from 50–250 atoms with a peak near 150 were seen in the FT-ICR cell even with a pulsed deceleration voltage of -800 V, which should have been sufficient to reject all supersonic carbon clusters with masses less than 43 000 amu ($C>3600$).

As we have argued elsewhere,[28] this unavoidable presence of carbon clusters in the range of 150 ± 100 atoms for carbon clusters whenever one is concentrating on larger carbon clusters is a consequence of the unique properties of fullerenes. When produced in rapidly condensing environments such as the laser vaporization nozzles featured here, these fullerenes are likely to aggregate. Since the chemical valences of the fullerenes have largely been fulfilled in the aromatic bonding of the six- and five-membered rings, these clusters aggregate primarily by loose van der Walls forces, and therefore readily disaggregate by evaporative processes triggered either by collisions as these aggregates are thermalized in the ICR cell, or simply by the residual

thermal excitation in the cluster aggregate as produced by the supersonic source.

We feature this carbon cluster FT-ICR mass spectrum here to demonstrate some of the subtleties involved with direct cluster injection to an FT-ICR apparatus. At our current level of experience, this is a unique exception to the rule of simple, predictable trapping of clusters produced by the source and only slightly slowed by the "magnetic mirror" effect of the fringing field of the superconducting magnet.

In some cases such as this example of carbon clusters it may still be of advantage to extract the cluster ions at right angles and inject an accelerated ion beam pulse into the FT-ICR trap.[4,8] This gives more control on the ions injected. With the compact source shown in Fig. 1, this would simply entail an additional turbopumped six-way conflat cross with a tilted extraction stack.[18,32]

B. Using the trapped ions

As a final demonstration of the vitality of this new apparatus we show the use of cluster ions injected and trapped in this new fashion to actually learn something new (aside from simple mass spectroscopy). The principle objective of metal and semiconductor cluster experiments with ICR techniques is not to measure their masses or abundances, but instead to use the ICR trap as something akin to a UHV surface science apparatus to probe the surface chemistry of these cluster species. Figure 5 shows an example of the use of this new apparatus to learn about the surface chemistry of germanium clusters.

Due to the many isotopes of germanium with substantial natural abundance there is quite an extensive range of masses present in the ICR cell as injected from the supersonic beam. As is evident in Fig. 3 these isotopomers leave very little baseline between peaks for adjacent clusters on which to look for reaction products. As seen in the top panel of Fig. 5, this initial distribution may be dramatically simplified by selectively sweeping some of the clusters from the cell. This technique, commonly known as "SWIFT" (stored waveform inverse Fourier transform),[33] involves the calculation of the inverse Fourier transform of the rf power spectrum needed to sweep selected ions from the ICR cell. The resulting time domain waveform is then generated by a fast 14-bit DAC, amplified and applied to the rf excitation plates of the ICR cell. In the case of Fig. 5 this SWIFT waveform was chosen so as to sweep out a clean baseline between the dominant isotopic components of the germanium clusters in the 39–46 atom size range.

The bottom panel of Fig. 5 shows the result of exposure of the selected clusters to nitric oxide gas at a pressure of 1×10^{-4} Torr for 10 s. Prior to the reaction the clusters had been thermalized to 300 K by roughly 2000 collisions with argon. For some clusters such as Ge_{43}^{+} reaction products of the form $Ge_{43}NO_{+}$ and $Ge_{43}(NO)_2^{+}$ are clearly seen, whereas other clusters such as Ge_{39}^{+} and Ge_{45}^{+} show no evidence of reaction at all. Similar results have been obtained for ammonia and ethylene reactions on positive silicon clusters[7,10,29] where again the 43rd cluster appears to be the most reactive and the 39th and 45th are inert. In

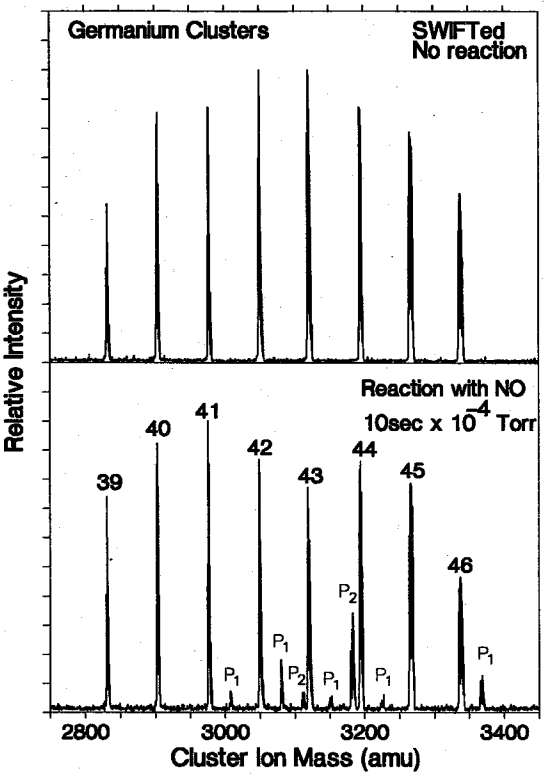

FIG. 5. Reaction study of Ge_x^{+} clusters with nitric oxide. The top panel shows the FT-ICR mass spectrum after selective removal of some ions from the cell by "SWIFT" excitation. The bottom panel shows this spectrum after exposure of the clusters to 1×10^{-4} Torr nitric oxide for 10 s at 300 K—roughly 30 000 collisions. Reaction products of the form $Ge_x(NO)_y^{+}$ have been labeled here as "P_y."

the case of silicon, laser annealing experiments have proved that the differences in reactivity are due to differences in surface structures.[30] The fact seen here in Fig. 5 that the same cluster reactivity pattern exists for germanium now provides evidence that germanium adopts the same structures as silicon in these small clusters.

Experiments such as these will benefit greatly from the new cluster source and the simplicity of direct injection.

IV. FUTURE APPLICATIONS

While our motivation in developing this new compact cluster beam source and the direct-injection FT-ICR apparatus has been to facilitate the study of metal and semiconductor clusters, it may have much wider applications. For example, the laser vaporization techniques of Cable *et al.*[34] or Karas *et al.*[35] for the study of large biomolecules are directly adaptable to the new compact supersonic beam source discussed above. Using either the ions produced in the vaporization event itself, or with an additional excimer laser ionization step in the emerging supersonic beam, direct injection into the FT-ICR apparatus should be just as straightforward with these large molecular species as demonstrated here with germanium clusters.

Somewhat less obvious is the extension of this compact laser vaporization beam source to molecular beam epitaxy (MBE).[36] Most modern MBE sources are effectively hot oven, effusive molecular beams. When used to prepare

complicated devices such as GaAs/AlGaAs heterostructures it is critical that these MBE sources provide stable, uniform fluxes of Al, Ga, and As (usually in the form of As_2 or As_4), and that these fluxes be controllable. With heated oven sources it is difficult to change the beam flux in a short period of time since the flux is dependent on temperature, and many minutes are required to stabilize operation at the new temperature setting. One of the advantages of an emerging new technique which uses metal organics[37] such as trimethylamine allane,[38] gallane, and arsene to produce beams for epitaxy (MOMBE)[36,37] is that far better control is available for the beam intensity and the Al/Ga ratio including very rapid on/off switching times. However, there are problems in attaining the requisite ultrahigh purity with these organometallics, and problems with controlling the surface chemistry so that contamination of the epitaxial surface with the organic component is minimized. In addition there are major problems of safety and long term environmental concerns in dealing with large amounts of volatile metal and arsenic compounds.

In this context, the new compact laser vaporization beam source shown in Fig. 1 has appealing qualities. By enlarging the critical "waiting room" region of the nozzle and opening up the diameter of the entrance orifice to the expansion cone, it is possible to virtually eliminate the formation of clusters while still efficiently entraining most of the vaporized metal or semiconductor atoms in the inert carrier gas, and accelerating this gas mixture to the terminal velocity of the supersonic beam. In fact we unintentionally explored this mode of operation prior to miniaturizing the nozzle dimensions. Generating intense, stable atomic beams of metals and semiconductors by laser vaporization is far easier than producing the germanium clusters seen in Fig. 3. With the careful attention already given to fine control of the target disk motion and the pulsed valve operation, this compact source would provide a reasonable starting design for a general purpose supersonic MBE source. The fact that laser vaporization is a completely general technique, applicable to all metals and semiconductors, and the fact that the source is completely under computer control with no background whatever when the nozzle is turned off, give this compact pulsed laser vaporization source intriguing possibilities in the future of MBE.

ACKNOWLEDGMENT

This research was funded by the Office of Naval Research for the study of semiconductor clusters, by the US Army Research Office for Gallium Arsenide cluster research, by the National Science Foundation for carbon cluster research, by the US Department of Energy, Division of Chemical Sciences for research on bare metal clusters, and by the Robert A. Welch foundation.

[1] R. T. McIver, Jr., R. L. Hunter, M. S. Story, J. Syka, and M. Labunsky, Proc. 31st ASMS Conf. Mass Spectrom. Allied Topics, Boston, MA, May 1983, pp. 44–45.
[2] U. S. Patent 4,535,235.
[3] J. M. Alford, F. D. Weiss, R. T. Laaksonen, and R. E. Smalley, J. Phys. Chem. **90**, 4480 (1986).
[4] J. M. Alford, P. E. Williams, D. J. Trevor, and R. E. Smalley, Int. J. Mass Spectrom. Ion Processes **72**, 33 (1986).
[5] P. Kofel, M. Allemann, H. Kellerhals, and K. P. Wanczek, Int. J. Mass Spectrom. Ion Processes **65**, 97 (1985).
[6] P. Kofel, M. Allemann, H. Kellerhals, and K. P. Wanczek, Int. J. Mass Spectrom. Ion Processes **72**, 53 (1986).
[7] J. L. Elkind, J. M. Alford, R. T. Laaksonen, F. D. Weiss, and R. E. Smalley, J. Chem. Phys. **87**, 2397 (1987).
[8] J. L. Elkind, F. D. Weiss, J. M. Alford, R. T. Laaksonen, and R. E. Smalley, J. Chem. Phys. **88**, 5215 (1988).
[9] J. M. Alford and R. E. Smalley, Mater. Res. Soc. Symp. Proc. **131**, 3 (1989).
[10] J. M. Alford, R. T. Laaksonen, and R. E. Smalley (unpublished).
[11] R. F. Curl and R. E. Smalley, Science **242**, 1017 (1988).
[12] M. P. Irion, A. Selinger, and R. Wendel, Int. J. Mass Spectrom. Ion Proc. **96**, 27 (1990).
[13] C. F. Ijames and C. L. Wilkens, J. Am. Chem. Soc. Mass. Spectrom. **1**, 208 (1990).
[14] G. Gabrielse, X. Fei, L. Orozco, R. Tjoelker, J. Haas, H. Kalinowsy, T. Trainor, and W. Kells, Phys. Rev. Lett. **65**, 1317 (1990).
[15] (a) T. G. Dietz, M. A. Duncan, D. E. Powers, and R. E. Smalley, J. Chem. Phys. **74**, 6511 (1981); (b) R. E. Smalley, Laser Chem. **2**, 167 (1983).
[16] R. E. Haufler, Y. Chai, and R. E. Smalley (unpublished).
[17] O. Cheshnovsky, K. J. Taylor, J. Conceicao, and R. E. Smalley, Phys. Rev. Lett. **64**, 1785 (1990).
[18] K. J. Taylor, C. L. Pettiette, O. Cheshnovsky, and R. E. Smalley (unpublished).
[19] G. I. Dimov, Pribory I Tekhnika Eksperimenta, Nuclear Physics Institute, Academy of Sciences of the USSR, No. 5, pp. 168–171 (1968).
[20] (a) W. R. Gentry and C. F. Geise, Rev. Sci. Intrum. **49**, 595 (1978); (b) W. R. Gentry, in *Atomic and Molecular Beam Methods*, edited by G. Scoles (Oxford University Press, Oxford, UK, 1988), pp. 64–66.
[21] (a) M. G. Liverman, S. M. Beck, D. L. Monts, and R. E. Smalley, Rarefied Gas Dynam. 11, 1037 (1979); (b) M. J. Liverman, S. M. Beck, D. L. Monts, and R. E. Smalley, J. Chem. Phys. **70**, 232 (1979).
[22] J. B. Hopkins, P. R. R. Langridge-Smith, M. D. Morse, and R. E. Smalley, J. Chem. Phys. **78**, 1627 (1983).
[23] PSV Pulsed Supersonic Valve, R. M. Jordan Company, Grass Valley, CA.
[24] Electroformed Nickel Skimmer, Beam Dynamics, Inc., Minneapolis, MN.
[25] P. Milani and W. A. deHeer, Rev. Sci. Instrum. **61**, 1835 (1990).
[26] D. A. Dahl, J. E. Delmore, and A. D. Appelhaus, Rev. Sci. Instrum. **61**, 607 (1990).
[27] See for example A. G. Marshall and F. R. Verdun, *Fourier Transforms in NMR, Optical and Mass Spectrometry* (Elsevier, Amsterdam, 1990).
[28] S. Maruyama, M. Lee, and R. E. Smalley, Z. Phys. D (in press).
[29] L. R. Anderson, S. Maruyama, and R. E. Smalley, Chem. Phys. Lett. (in press).
[30] S. Maruyama, L. R. Anderson, and R. E. Smalley, J. Chem. Phys. **93**, 5349 (1990).
[31] L. Wang, L. P. F. Chibante, F. K. Tittel, R. F. Curl, and R. E. Smalley, Chem. Phys. Lett. **172**, 335 (1990).
[32] C. W. S. Conover, Y. J. Twu, Y. A. Yang, and L. A. Bloomfield, Rev. Sci. Instrum. **60**, 1065 (1989).
[33] A. G. Marshall, T. C. L. Wang, and T. L. Ricca, J. Am. Chem. Soc. **107**, 7893 (1985).
[34] J. R. Cable, M. J. Tubergen, and D. H. Levy, J. Am. Chem. Soc. **110**, 7349 (1988).
[35] M. Karas, A. Ingendoh, U. Bahr, and F. Hillenkamp, Biomed. Environ. Mass Spectrom. **18**, 841 (1989).
[36] See for example M. A. Herman and H. Sitter, *Molecular Beam Epitaxy* (Springer, Berlin, 1989).
[37] C. R. Abernathy, A. S. Jordon, S. J. Pearton, W. S. Hobson, D. A. Bohling, and G. T. Muhr, Appl. Phys. Lett. **56**, 2654 (1990).
[38] W. L. Gladfelter, D. C. Boyd, and K. F. Jensen, Chem. Mater. **1**, 339 (1989).